STUDIES OF EXCITABLE MEMBRANES

I. Macromolecular Specializations of the Neuromuscular Junction and the Nonjunctional Sarcolemma

JOHN E. RASH and MARK H. ELLISMAN

From the Department of Molecular, Cellular, and Developmental Biology and the Department of Psychology, The University of Colorado, Boulder, Colorado 80302. Dr. Rash's present address is the Department of Cell Biology and Pharmacology, School of Medicine, University of Maryland, Baltimore, Maryland 21201

ABSTRACT

The neuromuscular junctions and nonjunctional sarcolemmas of mammalian skeletal muscle fibers were studied by conventional thin-section electron microscopy and freeze-fracture techniques. A modified acetylcholinesterase staining procedure that is compatible with light microscopy, conventional thin-section electron microscopy, and freeze-fracture techniques is described. Freeze-fracture replicas were utilized to visualize the internal macromolecular architecture of the nerve terminal membrane, the chemically excitable neuromuscular junction postsynaptic folds, and the electrically excitable nonjunctional sarcolemma. The nerve terminal membrane is characterized by two parallel rows of 100–110-Å particles which may be associated with synpatic vesicle fusion and release. On the postsynpatic folds, irregular rows of densely packed 110–140-Å particles were observed and evidence is assembled which indicates that these large transmembrane macromolecules may represent the morphological correlate for functional acetylcholine receptor activity in mammalian motor endplates. Differences in the size and distribution of particles in mammalian as compared with amphibian and fish postsynaptic junctional membranes are correlated with current biochemical and electron micrograph autoradiographic data. Orthogonal arrays of 60-Å particles were observed in the split postsynaptic sarcolemmas of many diaphragm myofibers. On the basis of differences in the number and distribution of these "square" arrays within the sarcolemmas, two classes of fibers were identified in the diaphragm. Subsequent confirmation of the fiber types as fast- and slow-twitch fibers (Ellisman et al. 1974. *J. Cell Biol.* **63**[2, Pt. 2]:93 a. [Abstr.]) may indicate a possible role for the square arrays in the electrogenic mechanism. Experiments in progress involving specific labeling techniques are expected to permit positive identification of many of these intriguing transmembrane macromolecules.

In vertebrate skeletal muscle fibers, four distinct membrane systems, the neuromuscular junction postsynaptic folds, the sarcolemma, the T system, and the sarcoplasmic reticulum, are morphologically and functionally differentiated for the initiation and regulation of contractile activity. Although it may be hypothesized that each possesses a characteristic complement of transmem-

brane "integral proteins" (Singer and Nicolson, 1972) which mediate the molecular events of excitability, conventional thin-section electron microscope studies have not permitted *in situ* visualization of the functional membrane molecules or the determination of differences in molecular architecture of the several membranes. However, with the development of the freeze-fracture technique (Steere, 1957; Haggis, 1961; Moor et al., 1961; and Moor and Mühlethaler, 1963), and the subsequent demonstration that the *internal molecular architecture* of cell membranes is exposed during the cleaving process (Branton, 1966), the feasibility of identifying and quantitating specific molecular components of complex, naturally occuring membranes has finally been realized (Pinto da Silva et al., 1971; Miller and Staehelin, 1973). Consequently, we have initiated freeze-fracture studies of vertebrate skeletal muscles, hoping to identify and characterize one or more of the integral proteins associated with chemosensitivity and electrogenesis. We now describe two classes of intramembrane particulate arrays, one of which probably corresponds to the acetylcholine receptor-ionophore complexes of the neuromuscular junction postsynaptic folds and a second which may correspond to one (or more) of the several molecules responsible for the electrogenic properties of the sarcolemma.

MATERIALS AND METHODS

Small strips of diaphragm, intercostal, gastrocnemius, soleus, and extensor digitorum longus muscles were obtained from normal adult male albino rats (400–600 g) fixed by whole body perfusion through the left ventricle or were obtained by direct biopsy from unanesthetized animals dispatched by cervical dislocation. To facilitate perfusion, the blood was replaced and clotting thus minimized by initially perfusing for up to 60 s with an aerated "rinse" solution consisting of Tyrode's solution containing 10 units/ml heparin with or without 0.1% procaine (final pH 7.2). (Several samples obtained after Nembutal narcosis or etherization were found to induce changes in the freeze-fracture images of the presynaptic membranes [see Streit et al., 1972]. Data concerning alterations after exposure to a variety of drugs will be presented in subsequent reports.) The perfusion fixative solutions, consisting of 2.5% glutaraldehyde in either Tyrode's solution, 0.16 M Sorenson's phosphate buffer, or 0.16 M cacodylate buffer (pH 7.2 adjusted after addition of all reagents) were administered through the same cannulae at a rate of about 70 ml/min for 3–5 min. While perfusion was in progress the desired muscles were quickly dissected free and placed in fixative for 1 h.

After fixation, the muscles were dissected into small bundles containing 5–10 fibers and stained for acetylcholinesterase (and perhaps nonspecific cholinesterase) activity by a method modified from Karnovsky and Roots (1964). The modified medium employed in our experiments for staining acetylcholinesterase (AChE) consisted of 0.1% acetylthiocholine iodide, 0.01 M sodium citrate, 0.002 M copper sulfate, 0.0003 M $K_3Fe(CN)_6$, plus 1.25% glutaraldehyde in Tyrode's solution, phosphate, or cacodylate buffer (final pH 6.5). At pH 6.5, 1–3 h are required to obtain "direct coloring" as described by Karnovsky and Roots (1964). However, heavy deposits of amorphous white material thought to be equivalent to the "copper thiocholine sulfate" of Koelle (1951) are formed within 30–45 min. (Since several other electron-dense reaction products may also be formed, elemental analysis must be completed before a definitive description of our modified staining procedure can be presented). When the neuromuscular junctions were faintly opalescent, very small samples (about 0.05 mm^3) containing either a few neuromuscular junctions (NMJ) or portions of fibers at selected distances from the neuromuscular junction were dissected free, slowly equilibrated to 30% glycerol, placed on brass mesh specimen supports, quickly frozen in liquid Freon 12 maintained at −150°C, and fractured and replicated at −103°C on a Balzers freeze-etch device (Balzers AG, Balzers, Principality of Liechtenstein). For one basic control, intact intercostal muscle fibers were fixed and frozen without exposure to anesthetics, heparin, stains, or glycerol. However, in replicas of even these very short fibers (1–2 mm in length), the disproportionately large volume of nonjunctional material resulted in only very rare fractures through the neuromusuclar junction region. Since we observed no major differences between the cleaved junctional fold membranes of the controls and those of the fixed, stained, and glycerol-treated preparations, the majority of the images presented in this report are from the latter group.

For additional controls, samples of intercostal, extensor digitorum longus (EDL), and soleus muscles were fixed by immersion fixation (cervical dislocation, no anesthetics or heparin) with and without glycerol as a cryoprotectant. All samples fixed before exposure to additional reagents (stains, drugs, or glycerol) yielded images essentially identical to those presented below. In samples exposed to various drugs before fixation, however, particle arrays and distributions often appeared altered or disrupted. A description of the drug-induced changes is beyond the scope of this initial descriptive report. (For a description of particle migration and aggregation following exposure of *unfixed* tissues to glycerol and dimethylsulfoxide, see McIntyre et al., 1973).

After being stained for AChE activity, samples that were to be examined by conventional thin-section electron microscopy were postfixed in 1% OsO_4, dehydrated in methanol series, and embedded in Epon-Araldite-

DDSA mixture as previously described (Fambrough and Rash, 1971). With our modified AChE staining procedure, conventional thin sections of specimens stained very briefly (about 5 min) reveal electron-dense, spherical granules deposited around or in association with small filaments normally present in the basement membrane matrix. After prolonged staining (1–6 h), the electron-dense reaction products become confluent but remain limited to the areas originally occupied by the spherical granules. (Because the electron-dense granules appear to be immobilized by the filaments, i.e. like beads on a string, diffusion of reaction products away from the site of enzymatic activity during the brief period of staining seems unlikely). To visualize the nonlipid (primarily protein) components of the junctional folds, additional samples were extracted with acetone-methanol solutions (according to Napolitano et al., 1967; and Rosenbluth, 1973) before embedding. Silver and gray sections were cut with glass or diamond knives on a Porter-Blum MT-2B Ultramicrotome (Ivan Sorvall, Inc., Newtown, Conn.), and poststained with methanolic uranyl acetate (see Stempak and Ward, 1964) and lead citrate (Venable and Coggeshall, 1965).

Sections and replicas were examined in a JEM-100B electron microscope at accelerating voltages of 60, 80, or 100 kV and photographed on Dupont Graphic Arts Film (E. I. DuPont de Nemours & Co., Wilmington, Del.) at original magnifications of 2000–250,000. In freeze-fracture micrographs, measurements of particle *diameters* were made at the bases of the electron-transparent "shadows" and were made from high magnification *negatives* ($> \times 60{,}000$), with a micrometer eyepiece. Particle *counts* were made from prints of $> \times 50{,}000$ final magnification. It should be noted that because the depth of focus in the electron microscope is much less than the conformational variation present in freeze-fracture replicas, adjacent areas within a single micrograph may vary from greatly underfocused to greatly overfocused. In one such instance (Fig. 3 *a*), we have presented an image as a montage of two near-focus micrographs.

RESULTS

Neuromuscular Junctions in Thin Section

After staining for acetylcholinesterase activity, specimens were oriented so that sections could be obtained parallel or perpendicular to the nerve terminus or to the myofiber axis. At low electron microscope magnifications, thin sections of neuromuscular junctions stained for 1 h are seen to contain dense deposits within the synaptic cleft, and within the perijunctional basement membrane to a distance of about 3–5 μm from the cleft (Fig. 1 *a*). Collagen fibers (CF) normally present within the matrix are surrounded by the electron-dense deposits, resulting in "negatively stained" circular or linear profiles (arrows). (A small amount of "nonspecific" staining is observed in the basement membranes at greater distances from the NMJ, but very little staining is observed within the myofiber or nerve terminal cytoplasms, or within intact satellite cells, fibrocytes, or the capillary endothelium.) At higher magnification (Fig. 1 *b*), the nature and extent of the deposits as well as the quality of tissue preservation can be assessed more accurately. Synaptic vesicles (SV), mitochondria, myofilaments, and elements of the sarcoplasmic reticulum (SR) seem minimally affected by the staining procedure. When stained very briefly (5 min) for AChE activity, however, the motor end-plate region is seen to contain numerous electron-dense granules (Fig. 1 *c*). At high magnification (Fig. 1 *d*) the spherical granules appear to be formed around, or entrapped by fine filaments of the basement membrane matrix. Staining for slightly longer periods results in apparent growth of the stain granules, and eventually, in virtually confluent deposits of electron-dense material (See Figs. 1 *a–d*). The regions containing highest cholinesterase activity are thus seen to occur in the basement membranes within 5 μm of the synapse. (Additional granules occasionally observed in the filaments of the basal laminae surrounding other cell types are presently attributed to the presence of nonspecific cholinesterase molecules associated with the filaments and not to lateral diffusion of granules.)

Freeze-Cleaved Neuromuscular Junctions

In freeze-fracture preparations, the cleavage plane passes preferentially within and along the hydrophobic lipid layers of the membranes, thereby producing large expanses of split membranes which are then replicated with platinum and carbon. In such replicas, the newly created surface representing the hydrophobic portion of the cytoplasmic leaflet is designated the "A face", whereas the split inner surface of the external or luminal leaflet is called the "B face." (For a detailed description of the cleaving process and the types of cleaving patterns produced, see Branton, 1966; and Benedetti and Favard, 1973.)

Fractures passing through the endplates normally expose large regions of the relatively smooth nerve terminal membrane (see Heuser et al., 1974), but only limited portions of the highly convoluted junctional folds. Occasionally, however, freeze-

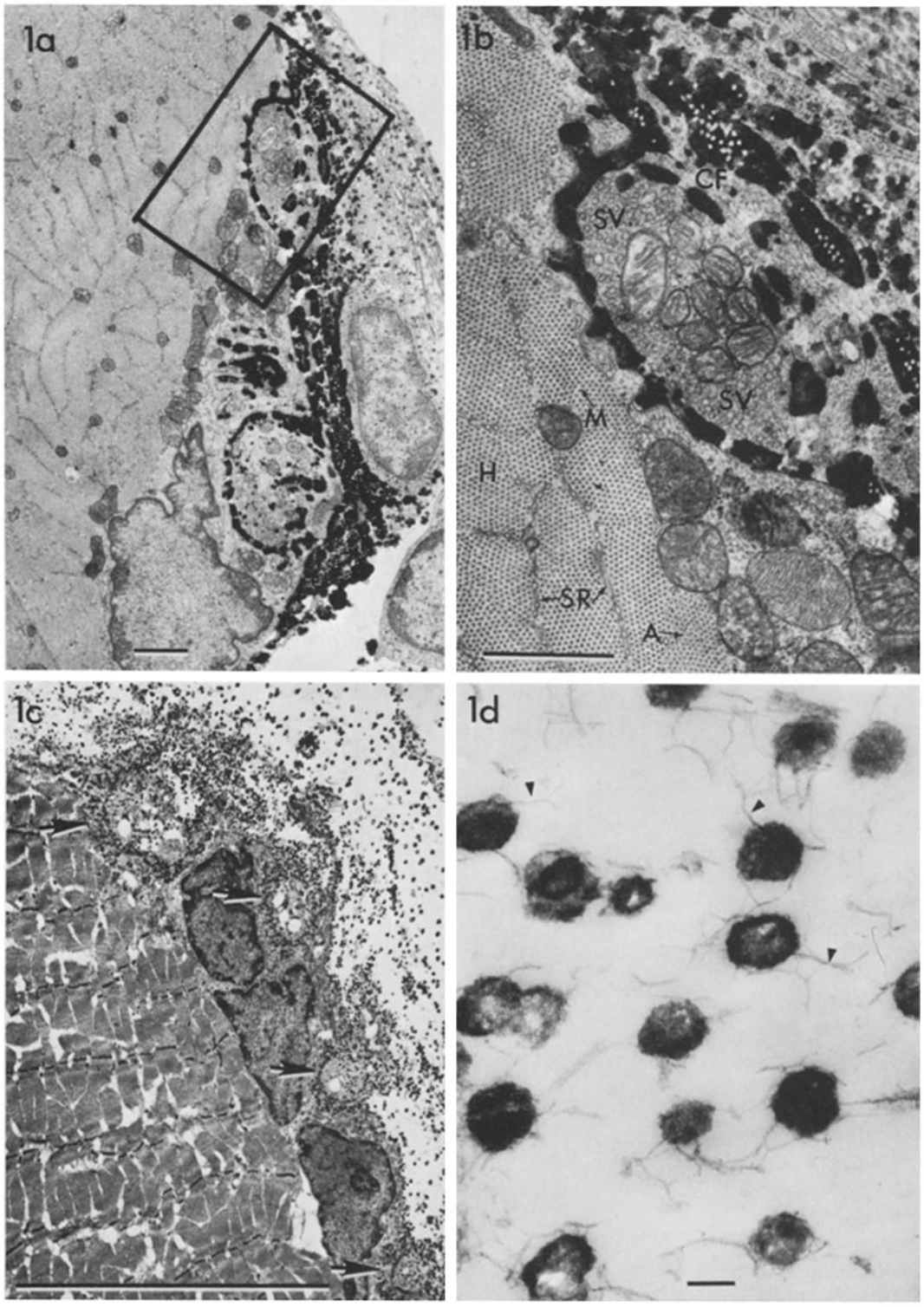
1a
1b
CF
SV
SV
M
H
SR
A
1c
1d

fracture images are seen which resemble images from thin sections (compare Fig. 2 *a* with Fig. 1 *a*). The cross-fractured nerve terminal (Fig. 2 *a*) contains numerous 500–700-Å synaptic vesicles, which appear either as small "bubbles" (the B face images) or as depressions (the A face images). Separating the neurolemma from the sarcolemmal junctional folds is the 500–800-Å wide synaptic cleft (SC). Mammalian nerve terminal A faces (Fig. 2 *b*) are easily recognized by the presence of characteristic double rows of four to eight 100-Å particles (Fig. 2 *b*; B face pits in Fig. 3 *a*). These parallel arrays appear to be localized directly opposite the cleft openings and may be equivalent to the much larger "presynaptic ridges" associated with synaptic vesicle fusion and release as recently described in frog neuromuscular junctions (Heuser et al., 1974. See also Dreyer et al., 1973.) In samples cleaved approximately parallel to the myofiber axis, the nerve cytoplasm may be cleaved away, thereby revealing the nerve terminal B face (Fig. 3 *a*) and the underlying junctional folds. The A face images of the juxtaneural portions of the folds reveal numerous 110–140-Å particles arranged in irregular rows. The rows of particles are usually perpendicular to the long axis of each fold and terminate abruptly at about 25% of the depth of the clefts (See Fig. 4 *a*, *b*). Counts of the 110–140-Å particles on the A faces of the juxtaneural portions of the folds reveal a packing density of 1,800–2,300/μm^2, with an average of 1,900–2,000/μm^2. (Total area counted about 1 μm^2, with estimates from an additional 5 μm^2 by inspection only. If corrected for the increase in surface area due to the curvature of the juxtaneural portions of the folds, the calculated value is about 1,700–1,800/μm^2). At 1,800/μm^2, the 110–140-Å particles occupy about 20% of the junctional fold surface area.

$$\frac{1{,}800}{\mu m^2} \times \frac{\pi d^2}{4} = \frac{1{,}800 \times \pi (120\ \text{Å})^2}{4\ \mu m^2} = \frac{0.20\ \mu m^2}{\mu m^2} = 20\%$$

Since the globular protein glutamate dehydrogenase has a molecular weight of 1,000,000 daltons and a diameter of about 130 Å (Lehninger, 1970), the molecular weight of the irregularly shaped 110–140-Å particles in the junctional fold A face would probably be somewhat less, perhaps 500,000 daltons. If these heterogeneous particles are "integral proteins" as defined by Singer and Nicolson (1972), they must comprise a major portion of the total membrane protein of the junctional folds, i.e., about 10^9 daltons/μm^2. (For comparison, rhodopsin [mol wt 40,000] comprises about 80–90% of the membrane protein of the rod outer segment [Heitzmann, 1972] and is present at an average packing density of 20,000/μm^2, also about 10^9 Daltons/μm^2.)

B face images of the juxtaneural portions of the folds are only infrequently encountered, perhaps because their extremely concave surfaces are seldom shadowed sufficiently for optimum stabilization. In the B face images of the folds (Fig. 3 *c*), regular patterns of pits are occasionally observed, probably representing the areas from which the A face particles were removed. Usually, however, the smaller B face pits are poorly resolved and appear as irregular "stippling" on the upper portions of the junctional folds (Fig. 4 *a*). Significantly, very few particles remain on the B faces of the junctional folds of glutaraldehyde-fixed samples, paral-

FIGURE 1 (*a*) Cross section of myofiber at the region of the motor endplate. Stained for AChE activity for 1 h. Electron-dense deposits in synaptic cleft and within basal laminae over nerve terminal branches. × 7,500. (*b*) Higher magnification of inscribed area in Fig. 1 *a*. Dense deposits within synaptic cleft, synaptic grooves, and the perijunctional basement membrane. Collagen fibers (*CF*) outlined in negative contrast. Synpatic vesicles (*SV*) are seen in the nerve terminus; myofilaments, mitochondria and elements of the sarcoplasmic reticulum (*SR*) in the myofiber cytoplasm (section through myofibril *H*, *M*, and *A* zones.) × 20,000. (*c*) Low-magnification micrograph of myofiber stained very briefly (about 10 min) for AChE activity. Not osmicated. (Lipids were extracted with methanol and acetone before embedding.) Granular deposits observed in synaptic clefts (arrows), in perijunctional basement membrane, and in association with nearby collagen fibers (not resolvable in this low-magnification micrograph.) × 5,000. (*d*) Higher magnification of spherical electron-dense deposits associated with thin filaments of the basement membrane matrix. (Fibers teased apart, resulting in partial disruption of basment membrane.) × 75,000.

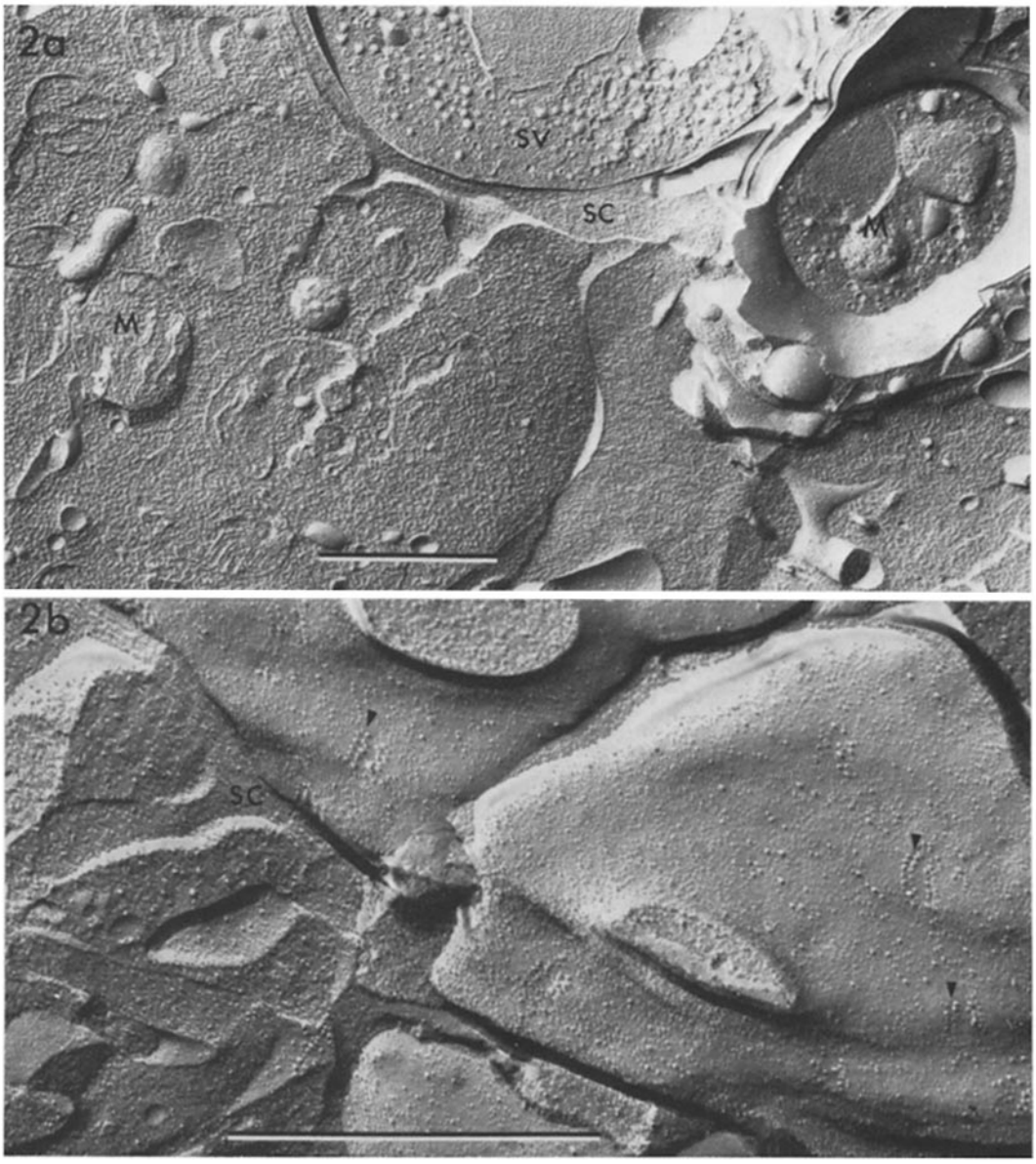

FIGURE 2 (*a*) Cross fracture through neuromuscular junction. Two branches of nerve terminal are exposed, revealing synaptic vesicles (*SV*) and the 500–1,000-Å wide synaptic cleft (*SC*). In the myofiber, cytoplasm mitochondria (*M*) are easily identified. Cleavage plane through edge of functional folds. × 25,000. (*b*) Neuromuscular junction revealing nerve terminal A face (*A*) with characteristic double rows of 100-Å particles (arrowheads), which are usually located opposite openings to junctional clefts (see Dreyer et al., 1973). × 50,000.

leling observations from fish electroplax and amphibian motor endplates (see Heuser et al., 1974). Since unfixed junctional folds have not been observed we cannot ascertain whether the pattern of A face particles and B face pits represents a natural structural anisometry or an artifact of fixation such as would result from cross linking transmembrane macromolecules to cortical cytoplasmic elements.

The distribution of A face particles is not

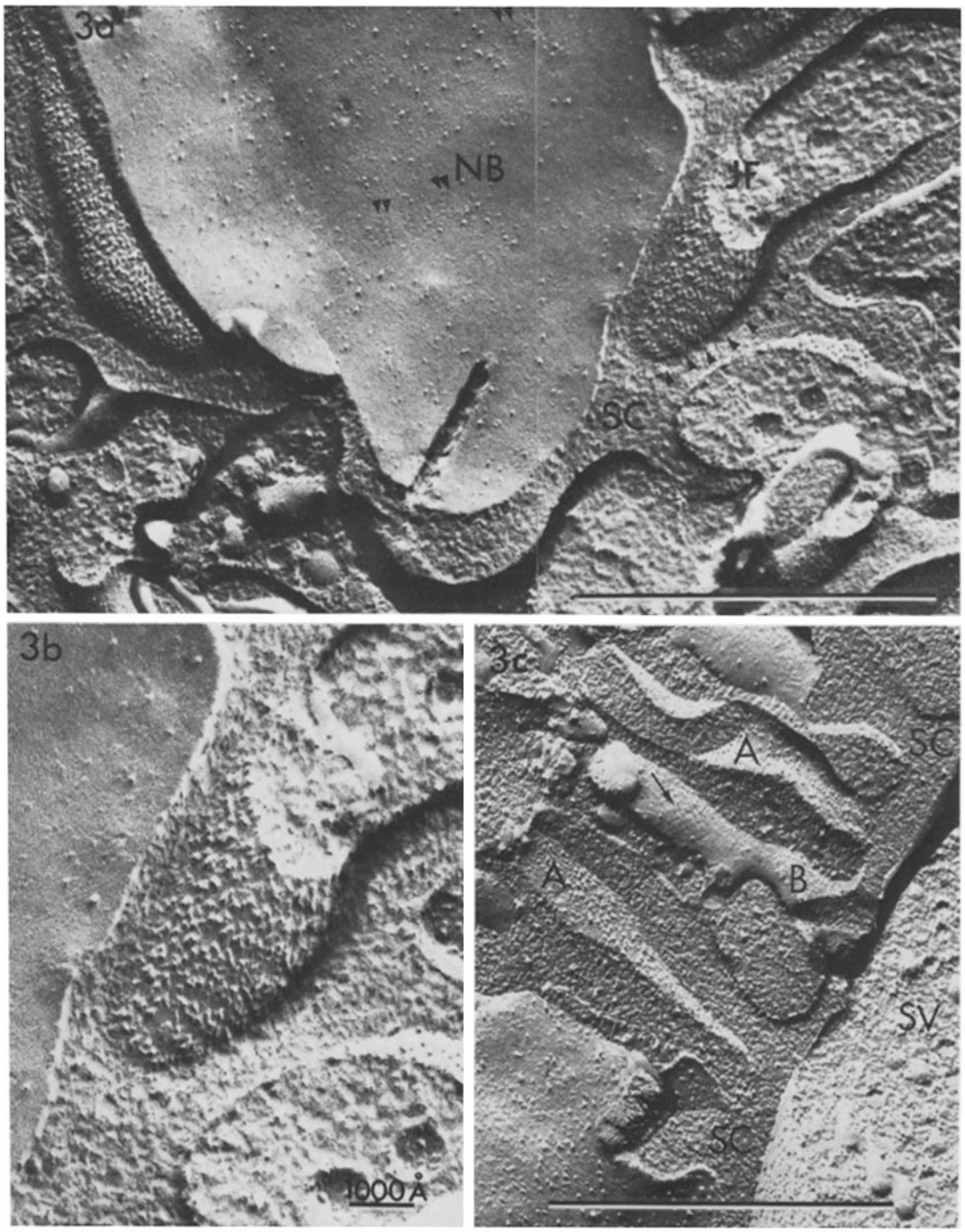

FIGURE 3 (*a*) Longitudinal fracture of a myofiber through the upper portions of the neuromuscular junction. The nerve cytoplasm has been cleaved away, thereby revealing the nerve terminal B face (*B*). Faintly resolved pits (arrowheads) representing the impressions of double rows of A face particles can be detected. The synaptic cleft (*SC*) contains a single included collagen fiber. The juxtaneural portions of several postsynaptic folds (*JF*) are exposed, revealing numerous 110–140-Å particles arranged in very irregular rows (arrowheads). (Illustrated at higher resolution in Fig. 5 *a*). × 55,000. (*b*) The irregular rows of 110–140-Å particles are present at a packing density of about 1,800/μm^2 and occupying about 20% of the split membrane surface. × 100,000. (*c*) Oblique fracture through NMJ. Particles observed on A faces (*A*) and occasionally regular arrays of pits on B faces (*B*). × 52,000.

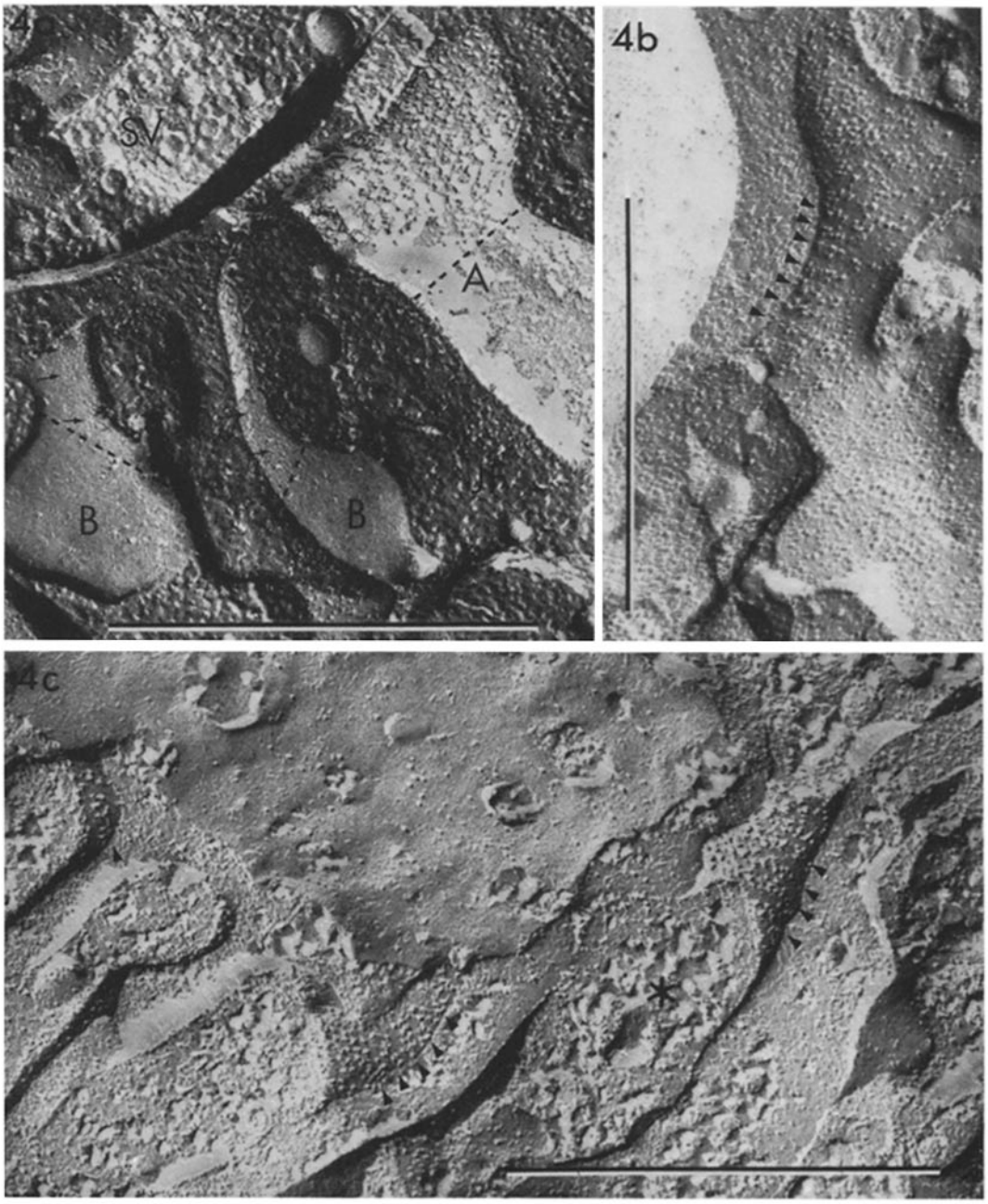

FIGURE 4 (*a*) Oblique fracture through two junctional folds. Because of the shadowing angle, the A face particle arrays are poorly resolved. The B face pits (arrows) appear as indistinct stippling. The irregular rows of particles and the poorly resolved B face pits terminate at about the level of the dotted line. × 60,000. (*b*) Oblique fracture exposing lateral surface of a split junctional fold. The rows of particles extend less than 25% of the depth of the fold, thus corresponding to the area occupied by the juxtaneural thickening (see Fig. 5 *b*, *c*). Irregularly scattered 80–140-Å particles (mostly 100 Å) are observed on the lateral walls and bottoms of folds (average packing density of about 500/μm^2). No inference is made that the juxtaneural and lateral wall particles are equivalent. × 60,000. (*c*) Mouse intercostal fixed briefly and frozen without staining or glycerination. Ice-crystal formation evident in cytoplasm (*). Irregular rows of particles (arrowheads) observed on tops of folds. State of aggregations of particles cannot be attributed to stains or cryoprotectants. × 60,000.

uniform over the entire surface of the junctional folds. The irregular rows of particles (and pits) terminate abruptly of the lateral walls at about 25% of the depth of the folds (Fig. 4 *a*, *b*), leaving only irregularly spaced particles of more varied diameters (80–140 Å) over the remaining lower 75% of the folds. Since the 80–140-Å particles in the lateral walls of the folds have a variable packing density of about 300–1000/μm^2 and the upper 25% of the folds has a packing density of about 2,000/μm^2, we estimate the average packing density of all particles (80–140-Å) to be about 1,000–1,200/μm^2 over the entire fold surface. A calculation of this nature, however, may be misleading, since recent electron microscope autoradiographs indicate that functional ACh receptors in mammalian neuromuscular junctions are confined almost exclusively to the juxtaneural portions of the folds (Fertuck and Salpeter, 1974, Albuquerque et al., 1974 *a*).

Artifacts of Specimen Preparation. Controls for Fixation, Staining, and Glycerination

Several recent reports have been presented which suggest the possibility of aggregation, migration, or alteration of particles observed in freeze-fracture preparations after exposure of samples to various common reagents, including anesthetics, common fixatives, cryoprotectants, solutions buffered outside the normal pH range, to prolonged exposure to temperatures above 4°C. or to physical trauma (see Streit et al., 1972; McIntyre et al., 1973; and Heuser et al., 1974). To ascertain if the morphology and state of aggregation of the A face particles might represent an artifact of our preparative procedures, we have examined samples prepared in each of the following ways: (*a*), mouse intercostal and rat diaphragm muscles were fixed very briefly by immersion fixation. Animals were sacrificed by cervical dislocation. No anesthetics, heparin, stains, or cryoprotectants were used (see Fig. 4 *c*); (*b*) rat diaphragm, extensor digitorum longus, and soleus muscles were fixed by perfusion. Animals were dispatched by cervical dislocation. Heparin and procaine were included in the initial perfusate. Specimens were processed with and without glycerol as a cryoprotectant; (*c*) rat and mouse diaphragms were fixed after general anesthesia (ether or Nembutal). Micrographs showing presynaptic alterations are not included in this initial descriptive report (see, however, Streit et al., 1972).

In the unstained, unglycerinated samples of intercostal muscle (control no. 1, Fig. 4 *c*), ice-crystal formation is evident in the cleaved cytoplasm (*). However, the characteristic 110–140-Å particles arranged in irregular rows (arrows) are evident in the replicated junctional fold A faces. We tentatively conclude, therefore, that the arrangement of the 110–140-Å particles into irregular rows is not an artifact of the staining or glycerination procedures. However, because we have been unable as yet to overcome the technical difficulties of obtaining freeze-fracture images of the endplate region of unfixed, unstained, unglycerinated myofibers, we cannot exclude the possibility either of particle aggregation during fixation or of an alteration of the cleaving pattern attributable to fixation.

Distribution and Morphology of A Face Particles. Correlation of Images from Freeze-Fracture Replicas and Thin Sections

Occasionally, replicas of branching junctional folds are obtained, each branch demonstrating irregular rows of particles arranged perpendicular to the fold axis. At high magnification the morphology, variability in size, and state of aggregation of the 110–140-Å particles are more easily visualized. (The thin white bridges apparently linking many particles are artifacts of focus due to a phase-contrast effect of slight underfocus.) It was assumed that if these 110–140-Å particles represent the ACh receptor and thus are protein, they could be visualized by ultrathin sectioning techniques, particularly if the lipid components of the membranes were extracted from the folds (see below).

In the original description by Birks et al. (1960), the membranes of the juxtaneural portions of the folds in mammalian motor endplates were shown to be of greater thickness and electron density than other cell membranes (See Fig. 5 *b*). By employing a variety of fixatives, Birks and coworkers were able to suggest that the membrane thickenings represent a dense accumulation of protein molecules, and they suggested that the acetylcholine receptor molecules and the acetylcholinesterase enzymes were the only two protein species present in the endplate region in sufficient quantities to

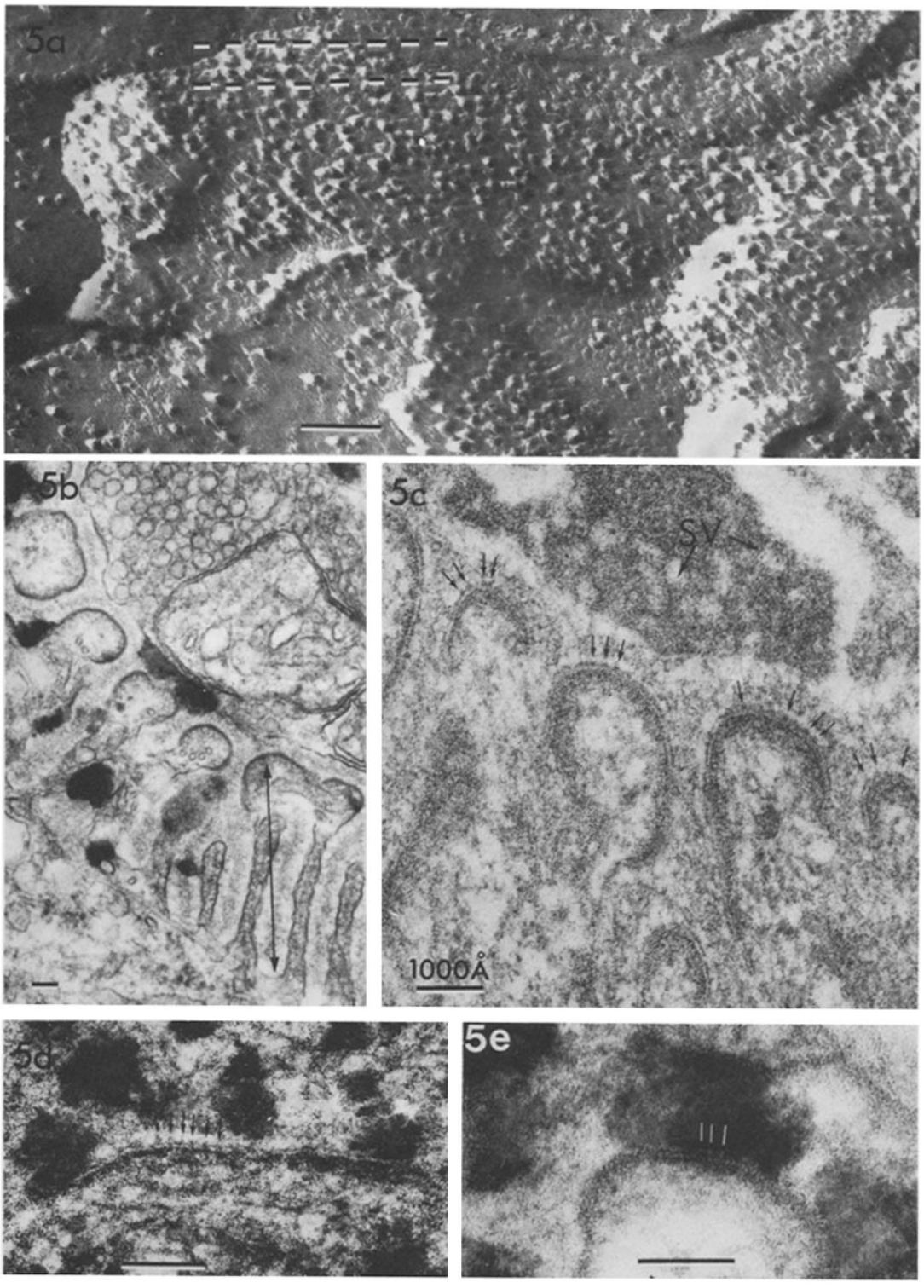
5a
5b
5c
SV
1000Å
5d
5e

account for the observed thickenings. While this manuscript was being revised, Fertuck and Salpeter (1974) published remarkable electron microscope autoradiographs clearly demonstrating that the ACh receptors of mouse motor endplates are confined to the juxtaneural portions of the folds; they concluded that the membrane thickenings, in fact, are composed almost exclusively of ACh receptor proteins. We have attempted further to characterize the junctional folds in thin sections and to identify the morphological correlates of the acetylcholine receptors by extraction techniques and enzymatic staining procedures. After glutaraldehyde fixation most proteins and glycoproteins are stabilized, thereby allowing the extraction of lipids with alcohol and acetone during dehydration and embedding (see Napolitano et al., 1967; and Rosenbluth, 1973). In high-magnification micrographs of the junctional fold membranes of lipid-extracted endplates (Fig. 5 *c*), irregularly spaced electron densities (arrows) can be observed in the juxtaneural thickenings described by Birks et al., (1960) and identified as the specific region of ACh receptor activity by Fertuck and Salpeter (1974), and Albuquerque et al., (1974 *a*). When the sections are tilted appropriately, additional periodic and aperiodic densities can be resolved, apparently from the exact registration and superposition of two (occasionally three) globular, non-lipid membrane subunits. (If stained properly, the 400–600-Å thick section would permit the superposition and visualization of two or three of the 110–140-Å particles described in this report. Exact spacing and resolution of the densities seen in thin sections would thus be functions of the section thickness, the orientation of the particle rows within the section, and the tilt of the section in the electron beam. [See dashed lines representing the thickness of a thin section in Fig. 5 *b*]). When clearly resolved, the densities have a center-to-center spacing of 160–300 Å and occasionally appear to extend from a dense cytoplasmic layer completely through the membrane and into the extracellular space (Fig. 5 *d*). When outlined in negative contrast by the AChE stain deposits (Fig. 5 *e*), additional aperiodic projections apparently emanating from (or closely associated with) the juxtaneural densities are observed extending approximately 150 Å into the synaptic cleft. These extracellular periodicities may represent an extension of the A face particles observed in freeze-fracture images of the junctional folds, or alternatively, additional molecules (such as AChE sites) attached to or closely associated with the junctional fold subunits.

The Electrically Excitable Nonjunctional Sarcolemma

Freeze-fracture preparations cleaved parallel to the myofiber axes in vertebrate striated muscle usually expose very large expanses of the split sarcolemmas. Previous reports describing the sarcolemma have been concerned primarily with demonstrating direct continuity of the T-system tubules with the sarcolemma and have not attempted to describe or characterize macromolecules exposed by the cleaving process (Bertaud et al., 1970; Rayns et al., 1968). In contrast, the present study is directed towards the elucida-

FIGURE 5 (*a*) Juxtaneural portion of a branching junctional fold. Rows of 110–140-Å particles are clearly evident. Dashed lines represent the thickness of a gray section (500 Å); the thickness and orientation of a section therefore would determine whether indvidual particles could be resolved and the number of particles superimposed. (All bars represent 1,000 Å or 100 nm). × 130,000. (*b*) Low-magnification micrograph of conventional thin section through motor endplate. Juxtaneural thickenings of junctional folds are clearly evident (double-ended arrow). (Glutaraldehyde, AChE stain, osmium tetroxide, uranyl acetate, lead citrate). × 40,000. (*c*) Lipid-extracted neuromuscular junction. Bilaminarity of membranes apparent only in portions of membranes with high protein content. In the juxtaneural portions of the folds, periodic and aperiodic densities (arrows) are observed projecting from the membrane outer leaflet (see analogous structures in insect myoneural junction, Rosenbluth, 1973.) Synaptic vesicles (*SV*) are visualized as indistinct areas of low electron density. × 105,000. (*d*) Lipid-extracted junctional folds with periodic densities (arrows), extending through membranea and into the synpatic cleft. Granular deposits from AChE stain are evident (greatly magnified from Fig. 1 *c*). × 130,000. (*e*) Juxtaneural portion of junctional folds lightly stained for cholinesterase. Macromolecules extending from fold surface are outlined in negative contrast (white bars). × 150,000.

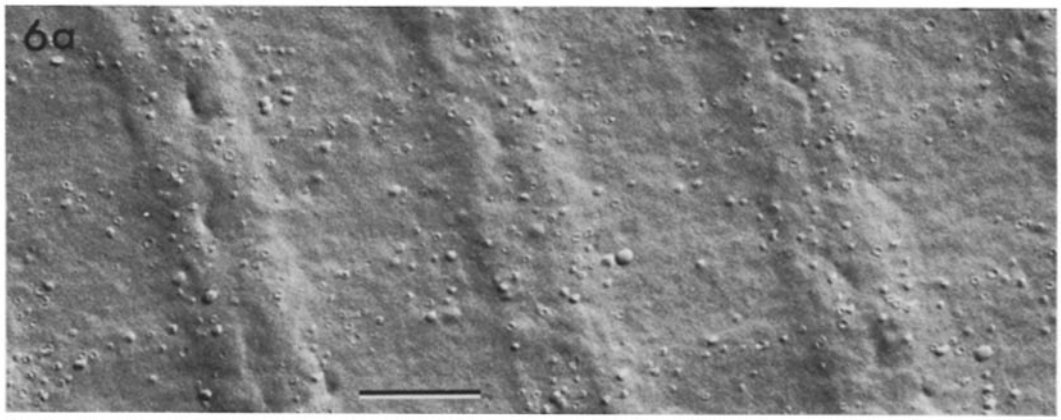
6a

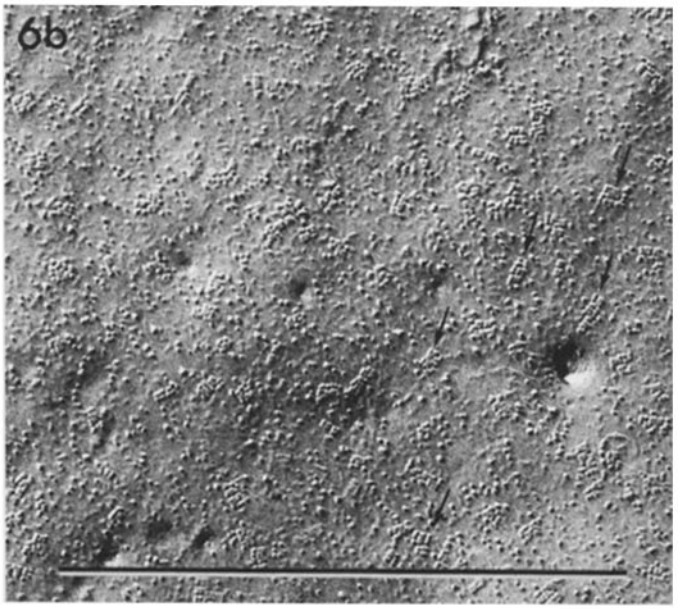
6b


6c
1000 Å

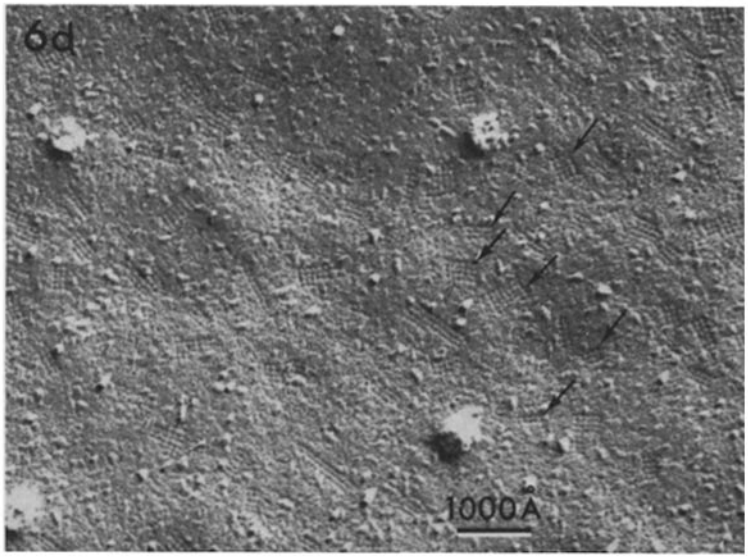
6d
1000 Å

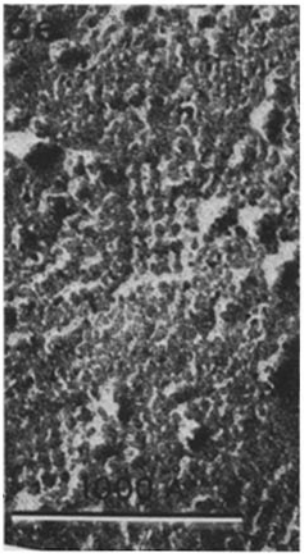
6e

tion of macromolecular details in relatively high-resolution replicas of the sarcolemma.

At low magnification, the sarcolemma appears as a fairly smooth expanse of membrane, marked at irregular intervals by the cross-fractured openings of cortical vesicles (Fig. 6 *a*) and, perhaps, T tubules. (We have been unable to identify positively the openings of T tubules, possibly because they are of small diameter and are not easily differentiated from the openings of the more numerous cortical pits and pinocytotic vesicles.) At higher magnification, close examination of the sarcolemma A faces reveals many orthogonal arrays of 60-Å particles with a center-to-center spacing of 70 Å (Fig. 6 *b*, *c*), while the complementary B faces reveal similar rectangular arrays of pits (Fig. 6 *c*, *d*). The number of subunit 60-Å particles in each of the orthogonal ("square") arrays varies from about 40 particles in the larger arrays to 3 or 4 in the smallest *recognizable* array, but numerous "singlet" and "doublet" 60-Å particles are also observed. Since the square arrays were observed in fixed and unfixed, stained and unstained, and glycerinated and unglycerinated fibers, the variability in the number of subunits per array may indicate the natural formation of paracrystalline aggregates in areas with high densities of a specific type of 60-Å particle. Areas (or whole cells) devoid of square arrays might then represent areas with subunit particles below a critical concentration. Experiments in progress are designed to test this hypothesis.

In previous reports (Rash et al., 1973 and 1974 *a*, *b*), we demonstrated that the square arrays do not represent a third type of gap junction, as was suggested for similar arrays in rat intestinal epithelium (Staehelin, 1972). In addition, square arrays have now been observed in human biceps myofibers (Rash, Ellisman, and Brooke, unpublished observations) and have been described in association with the postsynaptic folds of frog sartorius muscle (Heuser et al., 1974). Similar arrays also have been reported in brain astrocytes (Landis and Reese, 1974) and in hepatocytes (Kreutziger, 1968). In this initial attempt to characterize the square arrays, we have determined their number and distribution in the sarcolemmas of rat diaphragm myofibers by obtaining samples at selected distances from the stained neuromuscular junctions. (Because the NMJs in each dissected bundle are often misaligned by up to 0.5 mm, mapping to a greater accuracy than 0.5-mm increments in the nonjunctional samples is not possible by these methods. Future experiments will utilize mapping data obtained from individual fibers cleaved by the method of Pfenninger, 1972.) Analysis of particle counts at each distance from the NMJ reveals a nonuniform, nonrandom distribution of arrays, with at least two populations of fibers distinguishable. In the area immediately surrounding the NMJ, virtually no square arrays can be observed on any fibers. With increasing distance from the NMJ, however, the number of square arrays increases on many fibers, so that at about 500 μm (0.5 mm), the density of arrays is often greater than 50/μm^2 (see Fig. 6 *b*, *c*, *d*), corresponding to more than 1,000 subunit particles/μm^2 or 10^9 60-Å particles per mm^2. At 1,000 μm (1 mm) from the NMJ, many fibers have approximately 15–30 arrays/μm^2, while others possess virtually no square arrays. At 2 mm from the NMJ, fibers possess either about 10–20 arrays/μm^2 or $< 1/\mu m^2$; at 4 mm, either 10/μm^2 or $< 1/\mu m^2$; at 10 mm, either 5–10 or none; and at the myotendonal junction, either 5–20/μm^2 or none.

To determine if the difference in particle counts between adjacent fibers at 0.5, 2, 4, and 10 mm

FIGURE 6 (*a*) Low-magnification micrograph of freeze-cleaved sarcolemma. Contraction emphasizes the periodically spaced, paired mitochondria which surround the myofibrils at the level of the paired I bands. Openings of cortical vesicles not differentiable from the openings of T tubules. × 16,000. (*b*) Intermediate magnification of sarcolemmal A face revealing numerous orthogonal arrays of 60-Å particles. Density of arrays at 0.5–1 mm from the neuromuscular junction is approximately 30–40/μm^2. × 75,000. (*c*) High magnification of several "square" arrays, demonstrating 60-Å particles with a center-to-center spacing (square lattice) of 70 Å. Additional classes of 60–200-Å diameter particles are also present. × 175,000. (*d*) Intermediate magnification of split sarcolemma, demonstrating square arrays of complementary B face pits (arrows). Density of arrays at 0.5 mm from the neuromuscular junction is about 70/μm^2 in this micrograph. × 100,000. (*e*) High magnificant of square arrays of pits (B face images) resulting from splitting of membranes and adhesion of particle arrays to the A face. Additional classes of 60–200-Å B face particles are present. ×300,000.

could result from a highly asymmetric or patchy distribution at those distances, large areas (100–500 μm^2) of single fibers were surveyed. We never observed areas of low array density ($<1/\mu m^2$) and moderate or high array density ($>5/\mu m^2$) on the same fiber. Thus it seems likely that there are at least two populations of fibers in the diaphragm as determined by the number and distribution of square arrays, and that these differences may reflect subtle but measurable differences in basic membrane properties between the two fiber types. Since the diaphragm is a mixed muscle with both fast- and slow-contracting fibers, we have initiated a study of relatively pure populations of fast- and slow-twitch fibers as found in the extensor digitorium longus and soleus muscles, respectively. Preliminary data suggest that there are striking differences in the number and distribution of the square arrays in fibers from these fast- and slow-contracting muscles (Ellisman et al., 1974).

As a final observation, we note that many additional classes of particles (60–200 Å) are observed in both A and B faces of the sarcolemma (Fig. 6 *b–e*), but because they do not occur in distinct arrays, their characterization and quantification may be more difficult. A more detailed statistical analysis of the number and distribution of such particles is in preparation.

DISCUSSION

The Morphological Correlate for Acetylcholine Receptor Activity in the Mammalian Junction

In vertebrate striated muscle, the process of excitation-contraction coupling is initiated by the release of acetylcholine (ACh) from synaptic vesicles stored in the nerve terminal. (For recent reviews of the microphysiology of vertebrate neruomuscular transmission see Hubbard, 1973; Katz and Miledi, 1973; and DeRobertis, 1971.) The released ACh diffuses across the synaptic cleft and activates chemosensitive but electrically insensitive ion channels, the "ACh receptors," which are localized in complex infoldings of the postsynapatic membranes. Although many investigators have hypothesized that the receptors are uniformly dispersed over the postsynaptic junctional folds (see, for example, Fambrough and Hartzell, 1972) the recent reports of Fertuck and Salpeter (1974) and Albuquerque et al. (1974 *a*) present compelling evidence that the ACh receptors are localized almost exclusively in the thickened juxtaneural portions of the folds, as originally proposed by Birks et al. (1960). We have examined the junctional folds by freeze-fracture techniques and have observed a dense accumulation of 110–140-Å particles in the ACh receptor-rich juxtaneural thickenings. After lipid extraction from the junctional folds, the juxtaneural postsynaptic membrane thickenings were observed to consist of irregularly spaced electron densities with approximately the size and distribution of 110–140-Å A face particles. Thus it is proposed that the densities seen in thin sections and the particles seen in freeze-fracture preparations represent the same structure visualized by different means. Since the 110–140-Å particles seen in our freeze-fracture replicas of the motor endplate (*a*) are the only major class of particles (integral proteins?) present in the juxtaneural portions of the synaptic folds, (*b*) are confined to the areas which bind radioactive α-bungarotoxin (α-BgTx), and (*c*) are of the approximate dimensions predicted for the functional (high molecular weight) ACh receptor complex (see below), it is suggested that these particles represent the morphological correlate for functional ACh receptor activity in vivo. (Evidence has been presented that ACh receptors from *fish* electroplax are, in fact, membrane integral proteins and that they may be revealed by the freeze-fracture technique [Bourgeois et al., 1972, Cartaud et al., 1973]. Assumptions of similar properties for the mammalian ACh receptor seem warranted.)

Comparison of ACh Receptors from Fish, Amphibia, and Mammals

ACh receptors have been isolated and at least partially purified from a variety of vertebrate and invertebrate tissues. Until very recently the primary sources for purified ACh receptors have been the electric organs of *Torpedo* (electric ray) and *Electrophorus* (electric eel). When isolated from these sources, the partially purified ACh receptor complex has a molecular weight of 270,000 to 360,000 daltons (see Nickel and Potter, 1973; Cartaud et al., 1973; Eldefrawi and Eldefrawi, 1973) or even 500,000 daltons (Raftery et al., 1972). Despite disagreement as to the size of the functional complex, most investigators agree that the functional ACh receptor from these sources is composed of two to three ACh binding sites (mol

wt 90,000) or the equivalent four to six α-BgTx binding sites (mol wt 45,000) (see Cartaud et al., 1973; Meunier et al., 1972; Eldefrawi and Eldefrawi, 1973). Whether fixed or unfixed, the negatively stained or freeze-etched high molecular weight (270,000–360,000) ACh receptor complexes from *Torpedo* and *Electrophorous* have a diameter of 60–70 Å (Nickel and Potter, 1973) or 80–90 Å (Cartaud et al., 1973), and appear to be composed of about six subunits (α-BgTx binding sites?) of 20–25-Å diameter arranged around a central pore of about 15 Å diameter. In both fixed and unfixed membrane preparations, the irregularly shaped transmembrane proteins are densely packed (10,000/μm^2), with a center-to-center spacing of 80–90 Å (Nickel and Potter, 1973) or 90–100 Å (Cartaud et al., 1973).

Although ACh receptors from amphibian tissues have not been isolated or characterized biochemically, Heuser et al. (1974) have examined the postsynaptic membranes of frog neuromuscular junctions and have observed 80–120-Å particles tightly packed (6,000/μm^2) into small "islands" scattered over the junctional fold surface. (On the basis of our analysis of their micrographs, we estimate the *overall* packing density in the folds to be less than 3,000/μm^2).

ACh receptor complexes isolated from *mammalian* motor endplates have apparent molecular weights of about 550,000 daltons (Chiu et al., 1973; Kemp et al., 1973), or 50–100% larger than for ACh receptors isolated from fish electroplax. However, since the value of 360,000 mol wt reported by Meunier et al. (1973), for electroplax receptors had been corrected from 470,000 mol wt for detergent interaction, the value of 550,000 reported by Chiu et al. (1973), perhaps should be revised downward (Dolly, personal communication) to about 360,000–450,000 mol wt. Recently, these same investigators working in the laboratory of Barnard (Kemp et al., 1972–1973) using egg lecithin and the partially purified ACh receptor complex from mammalian skeletal muscle (apparent molecular weight of 550,000), reconstituted artificial bilayer membranes with functional ACh receptor activity (i.e., depolarization to applied ACh). Activity of the partially purified preparation was lost, however, when the high molecular weight complex was treated with strong detergents. In SDS, for example, the functional ACh receptor complex of about 500,000 mol wt appears to dissolve into four to six ACh-binding subunits (mol wt 90,000). Each of the 90,000 mol wt ACh receptors appears to have two α-BgTx sites, one at the actual ACh binding site and "protectable" by *d*-tubocurare, and a second at the "ionic conductance modulator" (ICM) site (see Chiu et al., 1974, and Albuquerque et al., 1973, 1974 *b*, *c*) which is not protectable by curare. Whether these two α-BgTx binding sites are on the same 90,000 mol wt molecule or are on different molecules of about 45,000 mol wt is not yet established (see Chiu et al., 1973; Albuquerque, Barnard, and Dolly, personal communications.)

Although precise values have not been established, it now seems evident that the functional AChR-ICM complex from mammalian motor endplates in vivo has a molecular weight of about 500,000 daltons, dimensions in excess of (100 Å)^3, and contains at least four to six ACh receptor sites (or 8–12 α-BgTx binding sites). Furthermore, the reported values of 60–70- and 80–90-Å diameter and packing density of 10,000 particles/μm^2 (or 33,000 BgTx binding sites, Bourgeois et al., 1972) observed in fish electroplax membranes and the 80–120-Å diameter and 6,000 (3,000?) particles/μm^2 observed in aldehyde-fixed amphibian motor endplates may now be contrasted with the 110–140-Å diameter and 1,800 particles/μm^2 observed in mammalian motor endplates. It is probable, therefore, that there are distinct differences in the sizes and packing densities of the ACh receptors in the endplates and electroplax of different vertebrate species.

Numerical Correlation of α-BgTx Binding Sites and Particle Packing Density

The 110–140-Å particles are of sufficient size to represent the ACh receptor but are present at a juxtaneural packing density of only 1,800/μm^2, far fewer than the overall average of 7,000–8,000 BgTx binding sites observed in mouse motor endplates (Salpeter and Eldefrawi, 1973; Porter et al., 1973 *a*, *b*, Albuquerque et al., 1974, *a*; Fertuck and Salpeter, 1974). When these *average* values are corrected for the observed juxtaneural distribution of BgTx binding sites (Fertuck and Salpeter, 1974), an even larger value of 21,000–32,000 binding sites/μm^2 would be predicted within the ACh receptor-rich juxtaneural portions of the folds. Since only 50% of the BgTx sites represent ACh receptor sites (the other half represent ICM sites, Albuquerque et al., 1974 *a*), the actual number of receptor sites is reduced to 10,000–16,000/μm^2. If each 110–140-Å particle

represents six to eight ACh receptor sites (mol wt 90,000 × 6 = 540,000), the 1,800 particles/μm^2 that we observed in the juxtaneural portions of the folds could account for the calculated number of receptors.

$$\frac{1{,}800 \text{ particles}}{\mu m^2} \times \frac{6 \text{ ACh receptors}}{\text{particle}} = 10{,}800 \text{ receptors}/\mu m^2,$$

or alternatively,

$$\frac{1{,}800 \text{ particles}}{\mu m^2} \times \frac{12\ \alpha\text{-BgTx sites}}{\text{particle}} = 21{,}600\ \alpha\text{BgTx sites}/\mu m^2.$$

We suggest, then, that sufficient circumstantial evidence has been assembled to implicate the 110–140-Å juxtaneural particles as the morphological correlate for functional ACh receptor activity in mammalian motor endplates. Positive identification, however, must await the application of direct freeze-fracture labeling techniques (see Fisher and Branton, 1973; and Miller and Staehelin, 1973). Preliminary exeriments to establish the efficacy of labeling with α-BgTx, curare, and cholinomimetic drugs are in progress.

Localization of Acetylcholinesterase Activity

Several investigators have proposed that acetylcholinesterase (AChE) molecules (mol wt 260,000, De Robertis, 1971; or mol wt 300,000–1,000,000, Dudai et al., 1973), may be closely associated with or may form an integral part of the neuromuscular junction postsynaptic membrane (cf. Birks et al., 1960; De Robertis, 1971). Since the 110–140-Å particles observed on the A faces of the folds in our preparations are of approximately the size to account for the observed molecular weight, it could be suggested that they represent AChE molecules. However, data from this and other laboratories suggest to the contrary. For example, Albuquerque et al. (1968), Hall and Kelly (1971), and Betz and Sakman (1971, 1973), have demonstrated that collagenase digestion of the basal laminae removes about 50% of the endplate AChE activity and that 85% of the solubilized AChE could be recovered enzymatically intact (Hall and Kelly, 1971). Since the basic electrical properties of the fiber (including resting potential, ability to propagate action potentials, and the duration of the rising phase of the endplate potential) were unaltered, AChE removal from within the plasma membrane matrix was considered unlikely. Significantly, the junctional folds remained and the membrane thickenings were not altered. However, a slightly prolonged depolarization response to applied ACh was observed and was attributed to the delayed diffusion of ACh from the clefts instead of the normal hydrolysis by acetylcholinesterase. Since the major change noted was the disappearance of the basal laminae and associated collagen fibers from the synaptic cleft, Betz and Sakman (1971, 1973), and Hall and Kelly (1971), concluded that the AChE molecules must be bound to the membrane exterior or to the material of the basement membrane. Our micrographs of sectioned material stained for AChE activity (see Fig. 1 *a–c*) demonstrate that most, if not all, of the endplate acetylcholinesterase- (and perhaps nonspecific cholinesterase-) staining products are bound to an unidentified filamentous component of the basement membrane matrix. Since the basement membrane matrix forms a very dense, netlike meshwork, diffusion of preformed granules is unlikely. Therefore, it is probable that the granules are initiated at the specific site of enzymatic activity and continue their accretion *in situ*. However, we cannot exclude the possibility that very small "nucleation centers" are formed at a different site (perhaps at the extracellular projections associated with the postsynaptic thickenings) and diffuse throughout the perijunctional basement membrane matrix until they are large enough to be trapped by the basement membrane matrix. Recently, we have applied our AChE staining procedures to murine muscular dystrophy (Bar Harbor strain 129/ReJ-dy) and have demonstrated the presence of the dense deposits within the perijunctional basement membranes. However, the deposits were not present within the clefts. Passive diffusion of reaction products could not account for the absence of stain deposits from the areas supposedly containing the highest concentrations of enzymes (the fold membranes). We tentatively concluded (Rash, et al., 1974 *a*, in press) that at least some isozymes of the acetylcholinesterase molecules are attached to or closely associated with the filamentous elements of the basement membrane matrix and that one or more isozymes may be missing from the cleft in murine dystrophy (see also Wilson et al., 1973). Experiments in progress are designed

to permit *in situ* visualization and quantification of the molecular sites of enzymatic activity.

The Molecular Basis for Electrical Excitability in the Sarcolemma

In response to the relatively large amount of ACh released from synaptic vesicles in an activated nerve terminal (see review by Hubbard, 1973, and the recent report by Katz and Miledi, 1973), several thousand AChR-ICM complexes are chemically activated (see Albuquerque et al., 1974 *b*, *c*). The resulting transient change in membrane permeability produces a depolarization called an "endplate potential" (EPP) which, subject to electrotonic decay, serves to trigger subsequent electrical events. Surrounding the NMJ is an area containing numerous currrent- or voltage-sensitive Na^+ channels (see Hille, 1970), which respond to the EPP by "opening" very briefly (about 10^{-5} s), thereby allowing the influx of about 1,000 Na^+ ions (see Katz and Miledi, 1973). Subsequently, the membrane permeability to K^+ ions reaches its maximum at separate K^+ channels (see Hodgkin and Huxley, 1952; and Hille, 1970). If the ionic current density (or change in transmembrane potential) reaches "threshold," adjacent channels are activated, and the result is the initiation and maintenance of the propagated "action potential." Since the sarcolemmal action potential can be initiated by direct electrical stimulation but not by directly applied ACh (Werman, 1960, 1963; Grundfest, 1966), the sarcolemmal "ionophores" ($Na^+/K^+/Ca^{++}$ channels, Hille, 1971; Reuter, 1973) can be contrasted with the nonspecific ionophores (AChR-ICM complexes) of the NMJ, which are chemically sensitive but electrically insensitive ion channels (see review by Reuter, 1973).

The chemically sensitive neuromuscular junction and the region immediately surrounding the endplate (about 100 μm wide) have been shown to be electrically "inexcitable" (Werman, 1960, 1963; Grundfest, 1966). These regions do not pass inward Na^+ current during a directly evoked muscle action potential (Werman, 1963) and presumably lack functional Na^+ channels. Furthermore, in the chemically excitable endplate, the Na^+ and K^+ conductances are not separable by pharmacological agents, whereas these opposing ion fluxes can be blocked independently in the electrically excitable (nonjunctional) portions of the sarcolemma (see Grundfest, 1966). Although limited electrophysiological evidence has been assembled, no morphological data are yet available to account for the localized differences in the electrogenic properties of the junctional and nonjunctional sarcolemma.

Although the evidence linking the square arrays with any functional molecule is at best circumstantial, we must note here that the square arrays are absent from (or present at a very low level in) the area corresponding to the perijunctional zone of electrical inexcitability but are present in large numbers in the surrounding electrically excitable portions of the sarcolemma. (It should be noted, however, that the square arrays have been observed in the electrically inexcitable region adjacent to the junctional folds of frog sartorius muscle [Heuser et al., 1974]). Nevertheless, our preliminary observations on fast- and slow-twitch muscle fibers (Ellisman et al., 1974) indicate that the square arrays are abundant in the sarcolemmas of fast fibers but *very* sparse in slow fibers, an observation which may be related to discrete but measurable differences in their membrane electrical properties (see Albuquerque and Thesleff, 1968).

Although the data are preliminary and subject to several interpretations, Albuquerque and coworkers (Albuquerque, personal communication) have obtained evidence for increased numbers of batrachotoxin binding sites in fast- vs. slow-twitch muscle fibers, with asymmetric spatial distributions similar to the distribution of square arrays on fast- vs. slow-twitch fibers. (Batrachotoxin is a frog neurotoxin which binds specifically and irreversibly to the Na^+ channels, see Albuquerque et al., 1971 *a*.) We are aware of no other data concerning the specific localization of Na^+ channels in vertebrate striated muscle fibers, nor of any data concerning the localization of the presumably closely associated K^+ and Ca^{++} channels. Nevertheless, we wish to call attention to this line of research and suggest that mapping of the various ion channel densities may provide especially valuable information concerning differences in the electrogenic mechanisms of fast- and slow-twitch muscle.

In addition to the ion channels, several other classes of transmembrane molecules occur in the sarcolemma. For example, maintenance of the ionic concentration difference responsible for the membrane resting potential requires active $Na^+/$

K^+ (and perhaps Ca^{++}) transport. The Na^+/K^+ ATPase molecules (or "pumps") expend energy to transport Na^+ ions from the cytoplasm to the external milieu, coupled with the transport of K^+ ions into the cytoplasm (see Eccles, 1964; Katz, 1966). Ultimately, these pumps expel approximately the same number of Na^+ ions that entered during the course of the action potential and replace the K^+ ions that were lost. At present, the distribution of Na^+/K^+ ATPase sites along the myofiber surface is not known, nor is the size of the purified Na^+/K^+ATPase molecule well established. (Preliminary data from freeze-fracture preparations of material supplied to us by Dr. Arnold Schwartz and Barry Van Winkle suggest a particle of about 100 Å significantly larger than the 60-Å particles of the square arrays.)

To continue our investigations of these intriguing square arrays, as well as the other particles described in this report, we have initiated freeze-fracture and thin-section analyses of their number and distribution in normal, chronically denervated and cross-innervated fast- and slow-twitch fibers (see Rash et al., 1974 *a*). By utilizing molecular labels specific for the Na^+ channels (batrachotoxin and tetrodotoxin, see Albuquerque et al. 1971 *a*, *b*; Narahashi, 1972), K^+ channels (tetraethylammonium and perhaps histrionicotoxin, see Albuquerque et al., 1974 *a*). Ca^{++} channels (Verapamil and D600, Knoll AG, Ludwigshafen a. Rh., W. Germany, see Baker et al., 1973), and Na^+/K^+ATPase (ouabain, see Baker and Willis, 1972; Chipperfield and Whittam, 1973), we hope to identify the square arrays and ultimately to employ similar techniques in the identification of other transmembrane macromolecules associated with specific electrochemical events of excitability and electrogenesis.

We wish to express our sincere appreciation to L. Andrew Staehelin for his continuing assistance in interpreting freeze-fracture micrographs and for the extensive use of his laboratory facilities, particularly his specially modified Balzers freeze-etch device. We also thank Professor Keith R. Porter for advice and consultation during the course of this investigation and in the preparation of this manuscript.

This work was supported in part by a fellowship (to John E. Rash) and a grant-in-aid (to Keith R. Porter and John E. Rash) from the Muscular Dystrophy Associations of America.

Received for publication 11 March 1974, and in revised form 10 June 1974.

REFERENCES

ALBUQUERQUE, E. X., E. A. BARNARD, T. H. CHIU, A. J. LAPA, J. O. DOLLY, S.-E. JANSSON, J. DALY, and B. WITKOP. 1973. Acetylcholine receptor and ion conductance modulator sites at the murine neuromuscular junction: evidence from specific toxin reactions. *Proc. Natl. Acad. Sci. U. S. A.* **70**:949–953.

ALBUQUERQUE, E. X., E. A. BARNARD, C. W. PORTER, and J. E. WARNICK. 1974 *a*. The density of acetylcholine receptors and their sensitivity in the postsynaptic membrane of muscle endplates. *Proc. Natl. Acad. Sci. U. S. A.* **71**:2818–2822.

ALBUQUERQUE, E. X., J. W. DALY, and B. WITKOP. 1971 *a*. Batrachotoxin: chemistry and pharmacology. *Science (Wash. D. C.).* **172**:995–1002.

ALBUQUERQUE, E. X., K. KUBA, and J. DALY. 1974 *b*. Effect of histrionicotoxin on the ionic conductance modulator of the cholinergic receptor: a quantitative analysis of the end-plate current. *J. Pharmacol. Exp. Ther.* **189**:513–524.

ALBUQUERQUE, E. X., K. KUBA, A. J. LAPA, J. DALY, and B. WITKOP. 1974 *c*. Acetylcholine receptor and ionic current modulator of innervated and denervated muscle membranes. Effect of histrionicotoxins. *In* Exploratory Concepts in Muscle (II) Control Mechanisms in Development and Function of Muscle and their Relationship to Muscular Dystrophy and Related Neuromuscular Diseases. Muscular Dystrophy Associations of America, New York. In press.

ALBUQUERQUE, E. X., M. D. SOKOLL, B. SONESSON, and S. THESLEFF. 1968. Studies on the nature of the cholinergic receptor. *Eur. J. Pharmacol.* **4**:40–46.

ALBUQUERQUE, E. X., and S. THESLEFF. 1968. A comparative study of membrane properties of innervated and chronically denervated fast and slow skeletal muscles of the rat. *Acta Physiol. Scand.* **73**:471–480.

ALBUQUERQUE, E. X., J. E. WARNICK, and F. M. SANSONE. 1971 *b*. The pharmacology of batrachotoxin. II. Effect on electrical properties of the mammalian nerve and skeletal muscle membranes. *J. Pharmacol. Exp. Ther.* **176**:511–528.

BAKER, P. F., H. MEVES, and E. B. RIDGWAY, 1973. Effects of manganese and other agents on the calcium uptake that follows depolarization of squid axons. *J. Physiol.* **231**:511–526.

BAKER, P. F., and J. S. WILLIS. 1972. Binding of the cardiac glycoside ouabain to intact cells. *J. Physiol.* **224**:441–462.

BENEDETTI, E. L., and P. FAVARD, editors. 1973. Freeze Etching: techniques and applications. Société Française Microscopie Electronique, Paris. 1–274.

BERTAUD, W. S., D. G. RAYNS, and F. O. SIMPSON. 1970. Freeze-etch studies on fish skeletal muscle. *J. Cell Sci.* **6**:537–557.

BETZ, W., and B. SAKMAN. 1971. "Disjunction" of frog neuromuscular synapses by treatment with proteolytic enzymes. *Nat. New Biol.* **232**:94–95.

BETZ, W., and B. SAKMAN. 1973. Effects of proteolytic enzymes on function and structure of frog neuromuscular junctions. *J. Physiol.* **230**:675–688.

BIRKS, R., H. E. HUXLEY, and B. KATZ. 1960. The fine structure of the neuromuscular junction of the frog. *J. Physiol.* **150**:134–144.

BOURGEOIS, J. P., A. RYTER, A. MENEZ, P. FROMAGEOT, P. BOQUET, and J.-P. CHANGEAUX. 1972. Localization of the cholinergic receptor protein in *Electrophorus* electroplax by high resolution autoradiography. *FEBS (Fed. Eur. Biochem. Soc.) Letters.* **25**:127–133.

BRANTON, D. 1966. Fracture faces of frozen membranes. *Proc. Natl. Acad. Sci. U. S. A.* **55**:1048–1056.

CARTAUD, J., E. L. BENEDETTI, J. B. COHEN, J.-C MEUNIER, and J.-P. CHANGEUX. 1973. Presence of a lattice structure in membrane fragments rich in nicotinic receptor protein from the electric organ of *Torpedo marmorata*. *FEBS (Fed. Eur. Biochem. Soc.) Letters* **33**:109–113.

CHIPPERFIELD, A. R., and R. WHITTAM. 1972. Reconstitution of the sodium pump from protein and phosphatidyl serine: features of ouabain binding. *J. Physiol.* **230**:467–476.

CHIU, T. H., J. O. DOLLY, E. A. BARNARD. 1973. Solubilization from skeletal muscle of two components that specifically bind α-bungarotoxin. *Biochem. Biophys. Res. Commun.* **51**:205.

CHIU, T. H., A. J. LAPA, E. A. BARNARD, and E. X. ALBUQUERQUE. 1974. Binding of *d*-tubocurarine and α-bungarotoxin in normal and denervated mouse muscle. *Exp. Neurol.* **43**:399–413.

DEROBERTIS, E. 1971. Molecular biology of snyaptic receptors. *Science, (Wash. D. C.).* **171**:963–971.

DREYER, F., K. PEPER, K. AKERT, C. SANDRI, and H. MOOR. 1973. Ultrastructure of the "active zone" in the frog neuromuscular junction. *Brain Res.* **62**:373–380.

DUDAI, Y., M. HERZBERG, I. SILMAN. 1973. Molecular structures of acetylcholinesterase from electric organ tissue of the electric eel. *Proc. Natl. Acad. Sci. U. S. A.* **70**:2473–2476.

ECCLES, J. C. 1964. The Physiology of Synapses. Springer-Verlag New York Inc., New York. 1-316.

ELDEFRAWI, M. E., and A. T. ELDEFRAWI. 1973. Purification and molecular properties of the acetylcholine receptor from *Torpedo* electroplax. *Arch. Biochem. Biophys.* **159**:362–373.

ELLISMAN, M. E., J. E. RASH, L. A. STAEHELIN, and K. R. PORTER. 1974. Freeze-fracture comparisons of the neuromuscular junction and post-junctional sarcolemmas of mammalian fast and slow twitch muscle fibers. *J. Cell Biol.* **63**(2, Pt. 2):93 a. (Abstr.).

FAMBROUGH, D., and C. HARTZELL. 1972. Acetylcholine receptor: number and distribution at neuromuscular junctions in rat diaphragm. *Science (Wash. D. C.).* **176**:189–191.

FAMBROUGH, D. and J. E. RASH. 1971. Development of acetylcholine sensitivity during myogenesis. *Dev. Biol.* **26**:55–68.

FERTUCK, H. C., and M. M. SALPETER. 1974. Localization of acetylcholine receptor by ^{125}I-labeled α-bungarotoxin binding at mouse motor endplates. *Proc. Natl. Acad. Sci. U. S. A.* **71**:1376–1378.

FISHER, K., and D. BRANTON. 1973. Freeze-fracture autoradiography: a method for studying biomembranes. *J. Cell Biol.* **59**(2, Pt. 2):99 *a* (Abstr.).

GRUNDFEST, H. 1966. Heterogeneity of excitable membrane: electrophysiological and pharmacological evidence and some consequences. *Ann. N.Y. Acad. Sci.* **137**:901–949.

HAGGIS, G. H. 1961. Electron microscope replicas from the surface of a fracture through frozen cells. *J. Biophys. Biochem. Cytol.* **9**:841–852.

HALL, Z. W., and R. B. KELLY. 1971. Enzymatic detachment of endplate acetylcholinesterase from muscle. *Nat. New Biol.* **239**:62–63.

HEITZMANN, H. 1972. Rhodopsin is the predominant protein of rod outer segment membrane. *Nat. New Biol.* **235**:114.

HEUSER, J. E., T. S. REESE, and M. D. LANDIS. 1974. Functional changes in frog neuromuscular junctions studied with freeze-fracture. *J. Neurocytol.* **3**:108–131.

HILLE, B. 1970. Ionic channels in nerve membranes. *Prog. Biophys. Mol. Biol.* **21**:3–32.

HODGKIN, A. L., and A. F. HUXLEY. 1952. Currents carried by potassium ions through the membrane of the giant axon of *Loligo*. *J. Physiol.* **116**:449–472.

HUBBARD, J. I. 1973. Microphysiology of vertebrate neuromuscular transmission. *Physiol. Rev.* **53**:674–723.

KARNOVSKY, M. J., and L. ROOTS. 1964. A direct coloring thiocholine method for cholinesterases. *J. Histochem. Cytochem.* **12**:219–221.

KATZ, B. 1966. Nerve, Muscle and Synpase. McGraw-Hill, Inc. New York. 1–193.

KATZ, B., and R. MILEDI. 1973. The binding of acetylcholine to receptors and its removal from the synaptic cleft. *J. Physiol.* **231**:549–574.

KEMP, G. J. O. DOLLY, E. A. BARNARD, and C. E. WENNER. 1972–1973. Reconstitution of a partially purified endplate acetylcholine receptor preparation in lipid bilayer membranes. *Biochem. Biophys. Res. Commun.* **55**:1044 (Reprint of 1972. **54**:607–613).

KOELLE, G. B. 1951. The elimination of enzymatic diffusions artifacts in the histochemical localization of cholinesterases and a survey of their cellular distributions. *J. Pharmacol. Exp. Ther.* **103**:153–171.

KREUTZIGER, G. O. 1968. Freeze-etching of intercellular junctions of mouse liver. *In* Proceedings of the 26th Meeting of the Electron Microscope Society of America. Claitor's Publishing Division, Baton Rouge, La. 234.

LANDIS, D. M. D., and T. S. REESE. 1974. Arrays of particles in freeze-fractured astrocytic membranes. *J. Cell Biol.* **60**:316–320.

LEHNINGER, A. L. 1970. Biochemistry, the Molecular Basis of Cell Structure and Function. Worth Publishers, Inc. New York. 29.

MCINTYRE, J. A., N. B. GILULA, and M. J. KARNOVSKY. 1973. Cryoprotectant-induced redistribution of intramembranous particles in mouse lymphocytes. *J. Cell Biol.* **59**(2, Pt. 2):208 *a* (Abstr.).

MEUNIER, J. C., R. W. OLSEN, and J.-P. CHANGEUX. 1972. Studies on the cholinergic receptor protein from *Electrophorus electricus*. Effect of detergents on some hydrodynamic properties of the receptor protein in solution. *FEBS (Fed. Eur. Biochem. Soc.) Letters* **24**:63–68.

MILLER, K. R., and L. A. STAEHELIN. 1973. Direct identification of photosynthetic enzymes on membrane surfaces revealed by deep-etching. *J. Cell Biol.* **59**(2, Pt. 2):226 *a* (Abstr.).

MOOR, H., and K. MÜHLETHALER. 1963. Fine structure in frozen-etched yeast cells. *J. Cell Biol.* **17**:609–628.

MOOR, H., K. MÜHLETHALER, H. WALDNER, and A. FREY-WYSSLING. 1961. A new freezing-ultramicrotome. *J. Biophys. Biochem. Cytol.* **10**:1–10.

NAPOLITANO, L., F. LEBARON, and J. SCALETTI. 1967. Preservation of myelin lamellar structure in the absence of lipid. A correlated chemical and morphological study. *J. Cell Biol.* **34**:817–826.

NARAHASHI, T. 1972. Mechanism of action of tetrodotoxin and saxitoxin on excitable membranes. *Fed. Proc.* **31**:1124–1132.

NICKEL, E., and L. T. POTTER. 1973. Fine structure of postsynaptic membranes in *Torpedo* electric tissue. *J. Cell Biol.* **59**(2, Pt. 2):246 *a* (Abstr.).

PFENNINGER, K. H. 1972. Freeze-cleaving of outgrowing nerve fibers in tissue culture. *J. Cell Biol.* **55**(2, Pt. 2):203 *a* (Abstr.).

PINTO DA SILVA, P., S. D. DOUGLAS, and D. BRANTON. 1971. Localization of A antigen sites on human erythrocyte ghosts. *Nature (Lond.)* **232**:194–195.

PORTER, C. W., E. A. BARNARD, and T. H. CHIU. 1973 *a*. The ultrastructural localization and quantitation of cholinergic receptors at the mouse motor endplate. *J. Membr. Biol.* **14**:383–402.

PORTER, C. W., T. H. CHIU, J. WIECKOWSKI, and E. A. BARNARD. 1973 *b*. Types and locations of cholinergic receptor-like molecules in muscle fibres. *Nat. New Biol.* **241**:3–7.

RAFTERY, M. A., J. SCHMIDT, and D. G. CLARK. 1972. Specificity of α-bungarotoxin binding to *Torpedo californica* electroplax. *Arch. Biochem. Biophys.* **152**:882–886.

RASH, J. E., M. H. ELLISMAN, and L. A. STAEHELIN. 1973. Freeze-cleaved neuromuscular junctions: macromolecular architecture of post-synaptic membranes of normal vs. denervated muscle. *J. Cell Biol.* **59**(2, Pt. 2):280 *a* (Abstr.).

RASH, J. E., M. H. ELLISMAN, L. A. STAEHELIN, and K. R. PORTER. 1974 *a*. Molecular specializations of excitable membranes in normal, chronically denervated, and dystrophic muscle fibers. *In* Exploratory Concepts in Muscle (II) Control Mechanisms in Development and Function of Muscle and Their Relationship to Muscular Dystrophy and Related Neuromuscular Diseases. Muscular Dystrophy Associations of America, New York. In press.

RASH, J. E., L. A. STAEHELIN, and M. H. ELLISMAN. 1974 *b*. Rectangular arrays of particles on freeze-cleaved plasma membranes are not gap junctions. *Exp. Cell Res.* **86**:187–190.

RAYNS, G. G., F. O. SIMPSON, and W. S. BERTAUD. 1968. Surface features of striated muscle. I. Guinea-pig cardiac muscle. *J. Cell Sci.* **3**:467–474.

REUTER, H. 1973. Divalent cations as charge carriers in excitable membranes. *Prog. Biophys. Mol. Biol.* **26**:1–43.

ROSENBLUTH, J. 1973. Membrane specialization at an insect myoneural junction. *J. Cell Biol.* **59**:143–149.

SALPETER, M. M., and M. E. ELDEFRAWI. 1973. Sizes of endplate compartments, densities of acetylcholine receptor and other quantitative aspects of neuromuscular transmission. *J. Histochem. Cytochem.* **21**:769–778.

SINGER, S. J., and G. L. NICOLSON. 1972. The fluid mosaic model of the structure of cell membranes. *Science (Wash. D. C.)*. **175**:720–731.

STAEHELIN, L. A. 1972. Three types of gap junctions interconnecting intestinal epithelial cells visualized by freeze-etching. *Proc. Natl. Acad. Sci. U. S. A.* **69**:1318–1321.

STEERE, R. L. 1957. Electron microscopy of structural detail in frozen biological specimens. *J. Biophys. Biochem. Cytol.* **3**:45.

STEMPAK, J. G., and R. T. WARD. 1964. An improved staining method for electron microscopy. *J. Cell Biol.* **22**:697–701.

STREIT, P., K. AKERT, C. SANDRI, R. B. LIVINGSTON, and H. MOOR. 1972. Dynamic ultrastructure of presynaptic membranes at nerve terminals in the spinal cord of rats. Anesthetized and unanesthetized preparations compared. *Brain Res.* **48**:11–26.

VENABLE, J. H., and R. A. COGGESHALL. 1965. A simplified lead citrate stain for use in electron microscopy. *J. Cell Biol.* **25**:407–408.

WERMAN, R. 1960. Electrical inexcitability of the synaptic membrane in the frog skeletal muscle fibre. *Nature (Lond.)*. **188**:149–150.

WERMAN, R. 1963. Electrical inexcitability of the frog neuromuscular synapse. *J. Gen. Physiol.* **46**:517–531.

WILSON, B. W., P. S. NIEBERG, C. W. WALKER, T. A. LINKHART, and D. M. FRY. 1973. Production and release of acetylcholinesterase by cultured chick embryo muscle. *Dev. Biol.* **33**:285–299.